

Sensitivity of Ice Storms in the Southeastern United States to Atlantic SST—Insights from a Case Study of the December 2002 Storm

RENATO RAMOS DA SILVA, GIL BOHRER, DAVID WERTH, MARTIN J. OTTE, AND RONI AVISSAR

Department of Civil and Environmental Engineering, Duke University, Durham, North Carolina

(Manuscript received 12 April 2005, in final form 19 September 2005)

ABSTRACT

Meteorological observations and model simulations are used to show that the catastrophic ice storm of 4–5 December 2002 in the southeastern United States resulted from the combination of a classic winter storm and a warm sea surface temperature (SST) anomaly in the western Atlantic Ocean. At the time of the storm, observations show that the Atlantic SST near the southeastern U.S. coast was 1.0°–1.5°C warmer than its multiyear mean. The impact of this anomalous SST on the ice accumulation of the ice storm was evaluated with the Regional Atmospheric Modeling System. The model shows that a warmer ocean leads to the conversion of more snow into freezing rain while not significantly affecting the inland surface temperature. Conversely, a cooler ocean produces mostly snowfall and less freezing rain. A similar trend is obtained by statistically comparing observations of ice storms in the last decade with weekly mean Atlantic SSTs. The SST during an ice storm is significantly and positively correlated with a deeper and warmer melting layer.

1. Introduction

Each winter extratropical cyclones impact the east coast of North America, and ice storms are among the most catastrophic of these events. During ice storms, snow or ice is created in a cold layer aloft, falls through a warmer layer (temperature $T > 0^{\circ}\text{C}$), melts, and then falls through a freezing layer near the surface, where the raindrops are cooled below freezing while remaining liquid. These supercooled raindrops freeze immediately on impact with exposed objects or the ground, creating an accumulation of ice (Zerr 1997). The weight of coated ice can cause trees and power lines to fall and roofs to collapse, resulting in widespread destruction (DeGaetano 2000; Changnon 2003a,b; Changnon and Karl 2003; Jones et al. 2004). These storms are usually associated with favorable meteorological conditions in conjunction with local surface characteristics, such as mountains and surface water bodies (Forbes et al. 1987; Martner et al. 1993; Szeto et al. 1999; Bernstein 2000; Gyakum and Roebber 2001; Robbins and Cortinas

2002; Roebber and Gyakum 2003). For instance, east of the Appalachian Mountains low-level cold air is transported from the north and remains trapped, a weather phenomenon known as “cold-air damming” (Bell and Bosart 1988). Approaching cyclones usually transport warm air northward above this cold layer at the surface, creating a melting layer that then produces freezing rain (Forbes et al. 1987).

In this paper, the atmospheric and oceanic conditions associated with the ice storm that took place in the southeastern United States in December 2002 are first analyzed as a case study. Second, the Regional Atmospheric Modeling System (RAMS) is used to simulate this storm and determine the sensitivity of accumulated freezing rain to changes in the Atlantic SST. This is the first time model and observation data are combined to search for an effect of SST on the intensity of ice storms. Last, we use SST and sounding observations from recent years to verify that the relationship seen in the sensitivity analysis exists for actual ice storms.

2. Case study: The December 2002 ice storm

On 4–5 December 2002 a severe ice storm affected the southeastern United States. Several locations in North and South Carolina recorded an accumulation of

Corresponding author address: Dr. Roni Avissar, Department of Civil and Environmental Engineering, 123 Hudson Hall, Duke University, P.O. Box 90287, Durham, NC 27708-0287.
E-mail: avissar@duke.edu

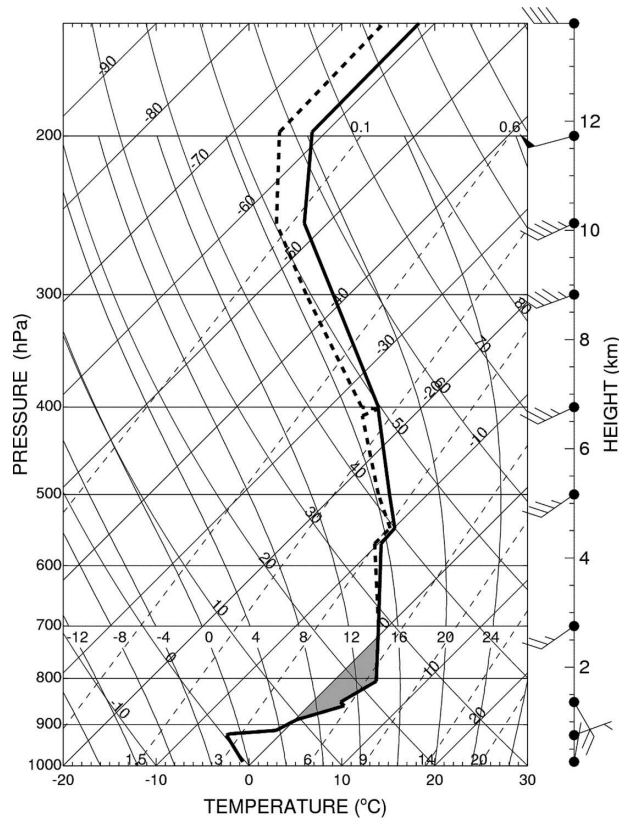


FIG. 1. Observed skew T thermodynamic profile at Greensboro, NC (36.08°N , 79.95°W), at 0600 UTC 5 Dec 2002. The boldface line indicates the temperature, and the dashed line indicates the dewpoint. The shaded area where the temperature is above 0°C indicates the MLI, and the vertical extent of this layer is the MLD. Long and short bars represent 10- and 5-kt wind speeds ($1 \text{ kt} = 0.5144 \text{ m s}^{-1}$), respectively. Data are obtained from the FSL/NCDC radiosonde archive of 6-hourly observation (available online at <http://raob.fsl.noaa.gov>).

freezing rain of more than 18 mm, causing many trees and power lines to collapse. The resulting damage was estimated at about 14 million dollars, and two million people were left without electricity for several days (Jones et al. 2004).

Figure 1 shows a thermodynamic skew T diagram from the radiosonde observation at Greensboro, North Carolina, at 0600 UTC 5 December 2002, corresponding to the time of intense local freezing rainfall. The profile shows a saturated melting layer ($T > 0^{\circ}\text{C}$) located between 800 and 2600 m that reached a maximum of about 5°C . In this warm layer snow fell from the cold layer above, melted, and then fell through the subfreezing layer near the surface, creating supercooled droplets. This profile also reveals that winds were from the west in the upper cold layer and from the southeast in the melting layer. Figure 2 displays the observed meteorological conditions at the time of the storm, based

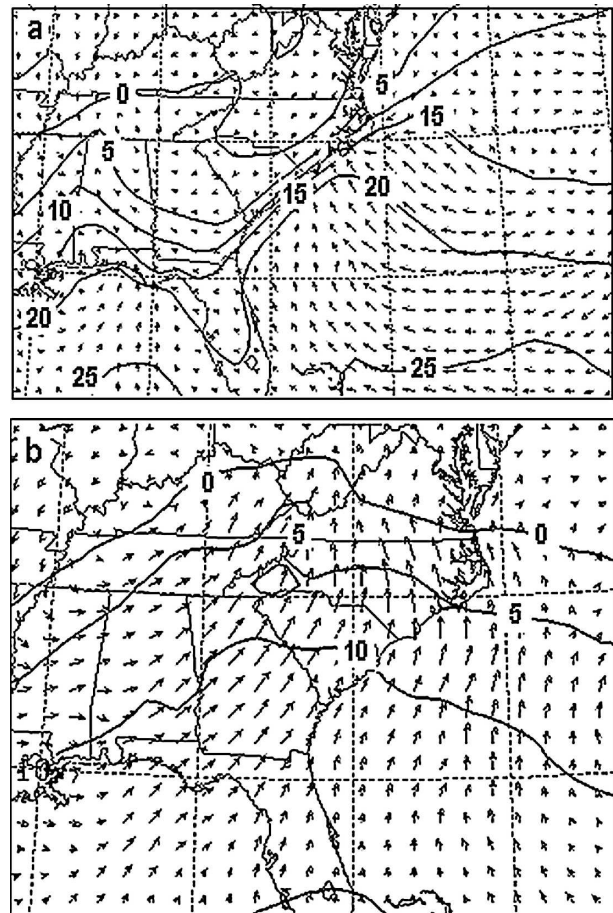


FIG. 2. Meteorological conditions at 0600 UTC 5 Dec 2002, obtained from the EDAS: (a) surface wind field and temperature ($^{\circ}\text{C}$) at 2 m above the ground, and (b) wind field and temperature ($^{\circ}\text{C}$) at 850 hPa. The longest wind vector corresponds to 13.75 and 25.0 m s^{-1} for (a) and (b), respectively.

on the Eta Data Assimilation System (EDAS). At that time, cold air was advected southward at low levels between the Appalachian Mountains and the Atlantic Ocean, leading to cold-air damming (Fig. 2a). The onshore winds over the Atlantic and Gulf of Mexico created a strong gradient of temperature between ocean and continent. At midlevels (850 hPa) a southerly flow advected warm, moist air from the Gulf of Mexico and the Atlantic (Fig. 2b). These meteorological conditions are commonly associated with winter storms along the east coast of the United States (Kocin and Uccellini 1990).

Figure 3 shows the SST anomalies obtained from the weekly optimal interpolation data (Reynolds et al. 2002) during the storm. This figure reveals a warm anomaly greater than 1.0°C in the western Atlantic off the southeastern U.S. coast, with the largest anomalies exceeding 1.5°C at about 26°N , 70°W . This anomalously warm region, in combination with the onshore

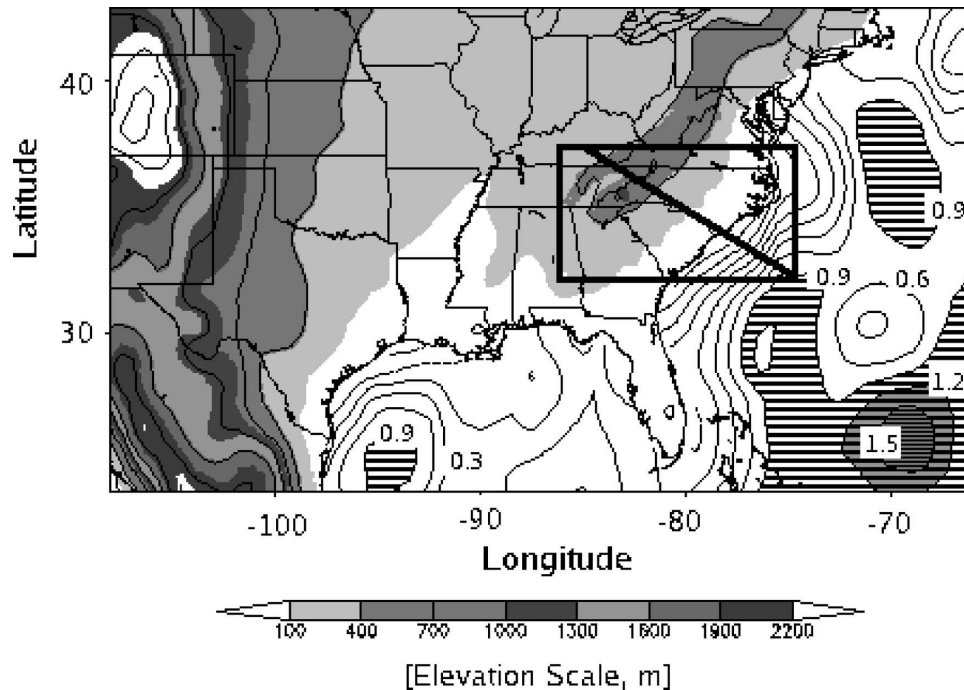


FIG. 3. Simulated domain, showing the 64-km (outer) grid along with the 16-km (inner) grid (black box). Sea surface temperature anomalies (degrees Celsius with values greater than 0.9 highlighted with stripes) for the period of 2–8 Dec 2002 are based on weekly means as described by Reynolds et al. (2002) (available online at <http://www.cdc.noaa.gov/cdc/data.oisst.V2.html>). The transverse line inside the box represents the location of the vertical cross section used in Fig. 6.

winds shown in Figs. 2a and 2b, was the main source of moisture and heat that produced the storm. Over the continent, this flow aloft transports heat and moisture into the melting layer as seen in the Greensboro southeasterly winds at 850 hPa within the melting layer (Fig. 1).

3. Sensitivity analysis

The RAMS model (Pielke et al. 1992; Walko and Tremback 2001) was used to investigate the effects of the Atlantic SST on the ice storm. RAMS is a three-dimensional model consisting of a set of prognostic equations, including dynamics, thermodynamics, and hydrometeor microphysics. These equations are solved numerically using finite-difference schemes applied to a staggered Arakawa C grid. The model contains several interacting submodels that simulate soil–vegetation–atmosphere exchange of heat and water (Avisar and Pielke 1989; Walko et al. 2000a); surface-layer turbulent processes (Louis 1979); boundary layer turbulent processes (Mellor and Yamada 1974); solar and thermal radiation transfer and its interaction with clouds (Harrington 1997); and cumulus cloud convection (Kuo 1974).

The cloud microphysics package in RAMS is very

detailed and has prognostic equations for the most prevalent hydrometeors (Walko et al. 1995; Meyers et al. 1997; Walko et al. 2000b). Therefore, the model can simulate the different types of winter precipitation. Water is partitioned in up to eight forms: vapor, cloud droplets, liquid rain, pristine ice, snow, aggregates, graupel, and hail. Cloud droplets and rain are liquid water, but may be supercooled. Pristine ice, snow, and aggregates are assumed to be completely frozen, while graupel and hail are mixed-phase categories, capable of comprising ice only or a mixture of ice and liquid. The model calculates the concentration of vapor in an atmospheric column and prognosticates the formation of different hydrometeors. Their size distribution is determined using a two-moment statistical scheme (Meyers et al. 1997). The model also follows the exchange of water and energy as hydrometeors interact with vapor and between each other (Walko et al. 2000b).

When hydrometeors are heavy enough (given their size and the vertical wind in the column) they fall and precipitate. Cloud droplets are assumed small enough to remain suspended, while all other categories do precipitate. Cloud droplets and pristine ice are the only categories to nucleate from vapor. All other categories form from existing hydrometeors. Once formed, how-

ever, they may also grow by vapor deposition. Pristine ice may also continue its growth by vapor deposition and is not permitted to grow by any other process. The definition of the pristine ice category is restricted to relatively small crystals, and larger pristine ice crystals are categorized as snow. The snow category is defined here as consisting of relatively large ice crystals that have grown by vapor deposition and riming. Together, the pristine ice and snow categories allow a bimodal representation of ice crystals. Aggregates are defined as ice particles that have formed by collision and coalescence of pristine ice, snow, and/or other aggregates. Like snow, aggregates are allowed to retain their identity with moderate amounts of riming. Pristine ice, snow, and aggregates are all low-density ice particles, having relatively low mass and fall speed for their diameters. Hail is a high-density hydrometeor, considered spherical in shape. It is assumed to be formed by freezing of raindrops or by riming or partial melting of graupel (Walko et al. 1995).

First, a control simulation for the December 2002 case study was produced and compared with observations. In this simulation, the model was set up using two nested grids: a coarse grid of 64×64 km² grid-size elements, which covers a large domain from the Rocky Mountains to the Atlantic Ocean, and a nested grid of 16×16 km² grid-size elements, which covers the region where most of the freezing rain was observed (Fig. 3). Atmospheric lateral boundary conditions are derived from the National Centers for Environmental Prediction–National Center for Atmospheric Research reanalysis project data (Kalnay et al. 1996). The SSTs were obtained from the weekly averaged optimum interpolation as described by Reynolds et al. (2002), and were kept constant during the simulation, which covered the period 3–6 December 2002.

In this work, we categorize liquid rain that falls where surface rain temperatures are below 0°C as freezing rain, and other liquid precipitation (where the surface rain temperatures are above 0°C) is considered as liquid rain. Snow, pristine ice, and aggregates are grouped as snow precipitation, and graupel and hail are grouped as ice pellets. Figure 4 shows the simulated accumulated precipitation for the period of the storm along with observations from several weather stations. Linear regression between the total measured precipitation at 116 stations in North Carolina east of longitude 83°W and the modeled total precipitation at the locations of those stations for the 3-day simulation yields a slope not significantly different than 1 (slope $\pm 95\%$ significance margins = 0.988 ± 0.040 , significance $P < 0.0001$, and correlation coefficient $r = 0.641$). Figure 5 shows that there was a good agreement between the simulated and

observed freezing rain and snow at Greensboro. The capability to simulate precipitation during the ice storm with RAMS is emphasized by these results.

A cross section from the RAMS simulation of the storm is given in Fig. 6. The cross section is oriented approximately parallel to the low-level southeasterly wind field ahead of the low pressure area. It shows the establishment of cold-air damming near the surface over land east of the Appalachian Mountains. There is a strong southeasterly flow in the lowest layers over the ocean, and this warmer air then advects up and over the shallow layer of cold air that exists over the land. Above the shallow cold layer there is a strong inversion, and the transport of warm air from the ocean just above this shallow cold layer is creating the melting layer.

Additional simulations were then performed assuming the exact same settings as in the case study (hereafter referred to as the “control” case), except for changes made to the prescribed Atlantic SSTs, where observed weekly mean SSTs for the week of 2–8 December 2002 offset everywhere by -4° , -2° , $+2^\circ$, or $+4^\circ$ C were used. In all other aspects, the simulation settings in all cases were identical. The results show that a warming of the Atlantic by 2° and 4° C increases freezing rain accumulation by 4.4% and 10.5%, respectively (Table 1). By contrast, decreasing the SST by 2° and 4° C causes a decrease of 2.3% and 2.6% in the amount of freezing rain, respectively, indicating the likelihood of a threshold, below which no further decrease of the melting layer could occur. The main reason for the increase in the freezing rainfall in the case of warmer SST is the presence of a deeper, warmer, and earlier-forming melting layer. Figure 7a shows that at 2100 UTC 4 December a warmer SST ($+4^\circ$ C) produces a melting layer that allows freezing rain to fall at Greensboro, while in the control case and with colder SSTs (-4° C), only snow falls because of the subfreezing temperatures at all heights (no melting layer exists at this time). Later, at 0400 UTC 5 December, the melting layer is about 1000 m deeper and the temperature is about 3° C warmer in the enhanced SST simulation ($+4^\circ$ C) in comparison with the cold SST case (Fig. 7b).

These results are consistent with observations that show the melting-layer depth associated with freezing rain formation in this region is between 1200 and 2700 m (Zerr 1997). Also, it is consistent with theoretical investigations that explain the ability of a deeper melting layer to convert more snow or ice into freezing rain (Zerr 1997). A shallower warm layer (as exists in the cold SST simulations) causes incomplete melting and the remaining ice becomes a nucleus for ice deposition. In this case, the supercooled drops refreeze before they

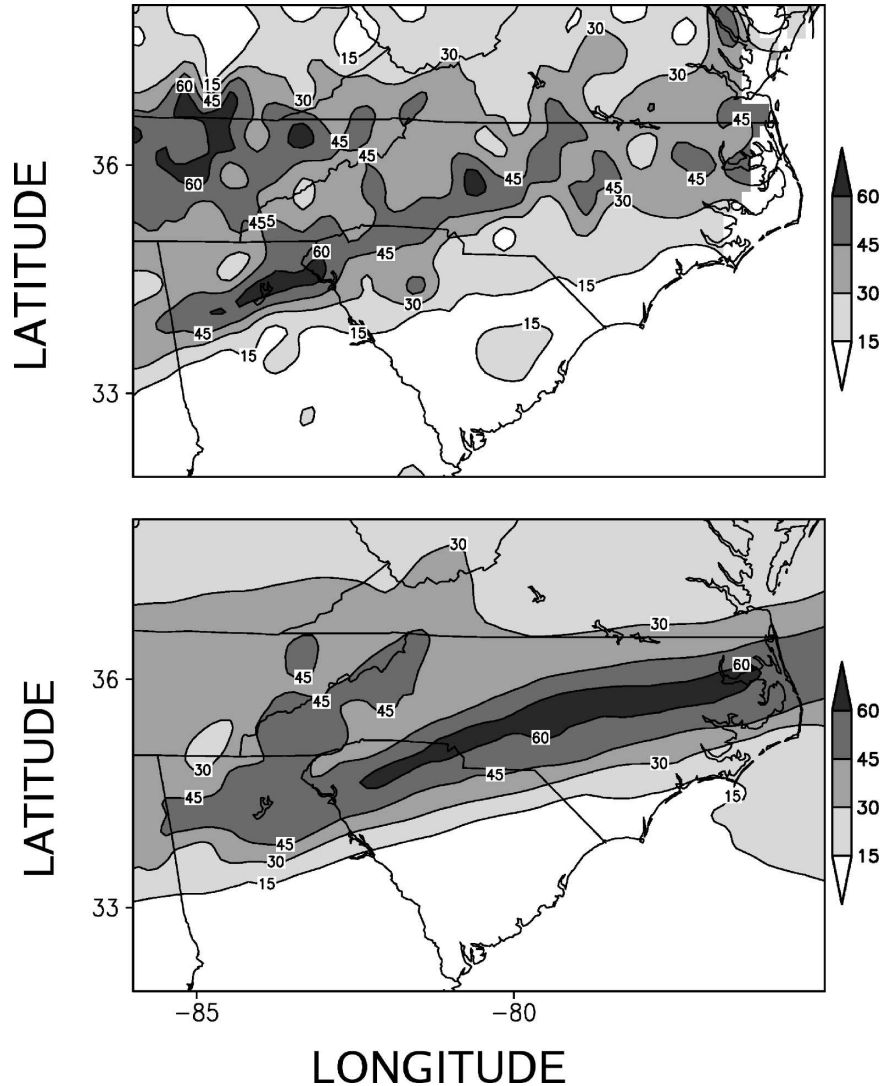


FIG. 4. (top) Observed precipitation (millimeters of equivalent water) from over 750 cooperative and National Weather Service observing sites for the period 3–7 Dec 2002, and (bottom) the accumulated precipitation (mm of equivalent water) simulated by RAMS from 1200 UTC 3 Dec to 1200 UTC 6 Dec 2002.

reach the surface and fall as ice pellets instead of freezing rain.

Using RAMS to simulate the different cases we find that increasing the SST leads to greater and earlier starting freezing rainfall (Fig. 5a). Conversely, decreasing the SSTs delays the onset of freezing rain, thus shortening the period of freezing rain precipitation, even though at some moments it was more intense than in the control case, and thus leading to reduced accumulation of ice (Fig. 5a). The reduced SST case leads to a longer period of snowfall, while the warmer SSTs caused snowfall to end sooner, at about the same time freezing rain started (Fig. 5b).

Evaporation increases with SST, but does not affect

the total precipitation (Table 1). Most of the changes occur in the southern United States where precipitation falls in liquid form (i.e., rainfall) and over the ocean where the evaporation changes occur (not shown). An analysis of the mean sensible heat flux from the ocean shows an increase of about 96% when SSTs are raised by 4°C and a decrease of about 46% when SSTs are lowered by 4°C as compared with the control simulation (Table 1). In these simulations, the higher heat flux causes larger amounts of liquid precipitation (rainfall) throughout the southeastern United States (not shown). Although there is a large increase in sensible heat flux as the Atlantic SST increases, the spatial area that experiences freezing rain does not increase with

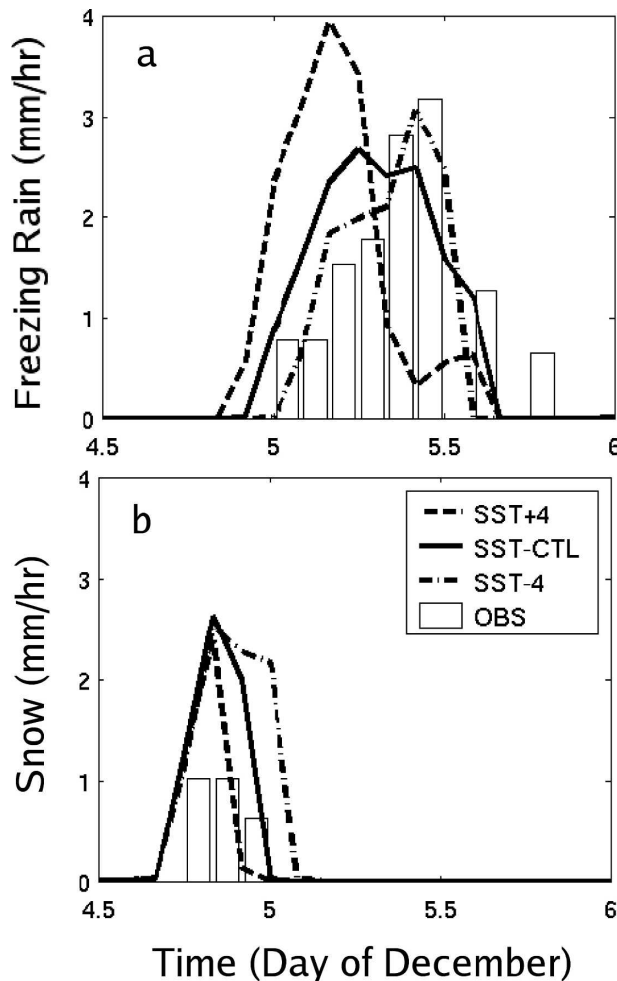


FIG. 5. Meteogram showing the time series of precipitation rate for (a) freezing rain and (b) snow at Greensboro, NC. The observations are given by the bars, the control simulations are given by the solid lines, and the +4 and -4 SST sensitivity simulations are given by the dashed and dashed-dotted lines, respectively.

the same magnitude (Fig. 8). The freezing layer in the lower part of the atmosphere (i.e., below 500 m) is not affected by SST because cold-air damming is controlled by topography and the continental synoptic frontal system. Indeed, further analysis of continental temperature fields (not shown) reveals no changes in their patterns in the sensitivity cases. For similar reasons, the general area over which a melting layer exists is rather constant in the storm domain as the SST varies (Fig. 8), but the depth of the melting-layer changes. The presence of a melting layer and a freezing layer below means that the area covered by freezing rain is relatively constant as the SSTs are altered (Table 1). But the relative intensities of freezing rain and snow are strongly affected (freezing rain positively and snow negatively) by the depth and temperature of the melt-

ing layer, which are affected by the SST forcing. The warmer scenario ($+4^{\circ}\text{C}$) results in a minor decrease of about 1% in freezing rain area, and the colder scenario (-4°C) results in an increase of about 3% (Fig. 8; Table 1). Therefore, in the warmer SST case, more freezing rain is produced over a similar area rather than expanding over a larger domain.

4. Comparison with historical data

To test whether the model case study results might extend to recent ice storms in the southeastern United States, atmospheric profiles of the last decade's winter storm events are compared with SST conditions. The atmospheric profiles were obtained from the National Oceanic and Atmospheric Administration (NOAA)/Forecast Systems Laboratory (FSL) database (<http://raob.fsl.noaa.gov/>). Stations were selected if they had data for the entire period of 1991–2004 (when storm data are available) and met the following criteria: they were located east of the Appalachians, were not at high altitude (below 760 m), and were not on the seashore. From these criteria, two stations were selected: Greensboro, North Carolina, and Sterling, Virginia.

The storm data were obtained from the National Climatic Data Center (NCDC) extreme weather and climate events database. Storms were selected based on reports from these two identified stations. These reports include snow, ice, and winter storms since 1991. Each station reports the time of peak precipitation and its category, such as freezing rainfall or snowfall. Storms that included both a snow period and a freezing rain period were classified as ice storms, and the storm time was the time of the ice period. Storms were omitted if it was impossible to separate the time of freezing rain from other precipitation types (rain, snow), or if information about the nature of precipitation of that storm in the station was missing.

Each storm was matched with the nearest radiosonde profile observation to create a storm-profile dataset. Cases in which no matching profile existed within 12 h of the storm time were not included in the storm-profile dataset. Given that most ice storms are short-lived and precipitate in the form of freezing rain over a limited time and area, the compiled storm-profile dataset includes large amounts of measurement noise, originated in measurements that were taken before, after, or outside the range of the ice storm. The SST observations used in this analysis were obtained from the NOAA weekly optimum interpolated database (Reynolds et al. 2002). The mean SST was computed for the area between latitudes 25° and 35°N and between longitudes 82° and 55°W and defined as a mean reference SST.

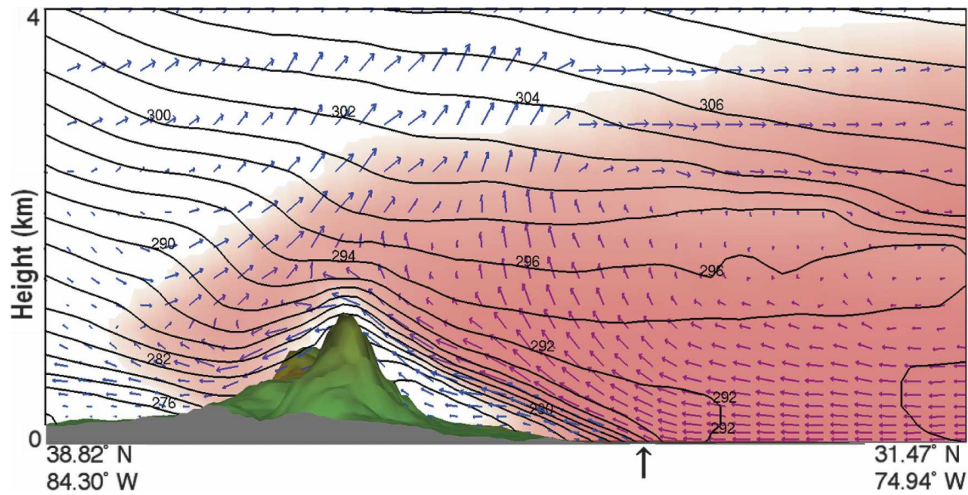


FIG. 6. Vertical cross section at 0600 UTC 5 Dec 2002 of potential temperature (K) and wind velocity along the cross-section line indicated in Fig. 3. The wind arrows are scaled to the aspect ratio of the plot with the largest arrows indicative of a horizontal wind speed of 15 m s^{-1} and a vertical wind speed of 0.2 m s^{-1} . Regions shaded red indicate air temperature greater than 0°C . The vertical arrow on the horizontal axis indicates the shoreline.

Each storm profile was matched to the reference SST of that week. Eventually, the storm-profile dataset included 68 storms, of which 27 were ice storms (Table 2). In general, ice storms happened when reference Atlantic SSTs were warmer. The mean (\pm one standard deviation) SST for ice storm events was $22.49^\circ \pm 0.17^\circ\text{C}$, while for snow storms it was $21.99^\circ \pm 0.14^\circ\text{C}$. This difference was significant (analysis of variance test, $P = 0.0218$).

Two meteorological variables conducive to ice storm development are melting-layer depth (MLD) and the melting-layer integral (MLI). The MLD is defined as the distance (km) in the sounding profile between the bottom and the top of the layer in which $T > 0^\circ\text{C}$. This depth has been found to be important in determining the amount of freezing rain (Zerr 1997). MLI ($\text{km } ^\circ\text{C}$) is defined as the vertical integral of positive melting layer temperature (i.e., the area of the positive part of the curve describing temperature versus height as illustrated in Fig. 1). It was calculated by numerical inte-

gration (using the trapezoidal method) of the radiosonde observation points in the melting layer. In both depth and profile, a linear interpolation was used to find the approximate start and end points of the profiles. Both MLD and MLI (in cases where those were greater than 0) were roughly an order of magnitude larger in ice storms in comparison with snowstorms (Table 2). The MLD proved to be a consistent indicator for the difference between ice and snowstorms; 70% of ice storms had a melting-layer depth greater than zero compared with only 15% of snowstorms (Table 2). This fact is a good indicator for the consistency of the storm-profile dataset, despite the expected high levels of noise that it includes. In this analysis, we excluded all ice storms in which an MLD did not exist in our dataset ($\text{MLD} = 0$). The ice storm events without a melting layer are probably the result of a time mismatch between the moment at which the radiosonde was launched and the time in which the storm produced freezing rain at the exact location of the radiosonde

TABLE 1. RAMS-simulated impacts of SST anomalies on freezing rain averaged over the inner domain. Percent change from the control case is given in parentheses. Sensible heat flux and evaporation are averaged in the ocean areas shown in Fig. 3.

Imposed SST anomaly ($^\circ\text{C}$)	Accumulated freezing rain (mm)	Tot precipitation (mm)	Max area covered by freezing rain (km^2)	Sensible heat flux (W m^{-2})	Evaporation (W m^{-2})
-4	13.73 (-2.6%)	34.4 (-0.6%)	565 248 (+3.4%)	10.46 (-46.3%)	1.40 (-48.0%)
-2	13.77 (-2.3%)	34.2 (-1%)	543 232 (-0.7%)	13.38 (-31.3%)	1.92 (-28.9%)
0	14.09	34.6	546 816	19.48	2.70
+2	14.71 (+4.4%)	34.2 (-1%)	539 904 (-1.2%)	27.70 (+42.2%)	3.72 (+37.8%)
+4	15.57 (+10.5%)	34.5 (-0.3%)	538 880 (-1.4%)	38.30 (+96.6%)	5.00 (+85.1%)

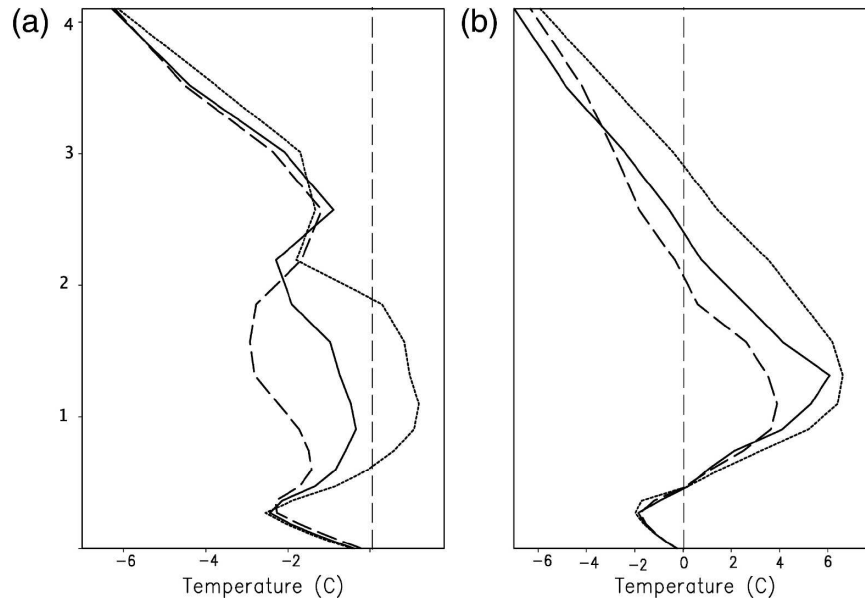


FIG. 7. Profiles of air temperature ($^{\circ}\text{C}$) for the control simulation (continuous line), and for the simulations with the Atlantic SSTs perturbed -4°C (dashed line) and $+4^{\circ}\text{C}$ (dotted line) near Greensboro, NC (35.5°N , 79.9°W) at (a) 2100 UTC 4 Dec 2002 and (b) 0400 UTC 5 Dec 2002.

station. Thus, this time mismatch may induce errors in the comparisons. Other sources of error arise from the fact that weekly mean SST was calculated using calendar weeks, regardless of the storm time. Also, small measurement errors of the radiosonde might cause large errors in the profile depth when the profile is nearly isothermal and close to 0°C .

All of the ice storms that had a MLD were correlated with the reference Atlantic SST. Scatterplots are created to show how the MLD and MLI vary with SST among the different storms (Fig. 9). The observed December 2002 ice storm is the strongest storm in the storm-profile dataset (it has the greatest MLI and MLD). Linear regression tests show a significant correlation between MLD and Atlantic SST (Fig. 9a), and also between MLI and Atlantic SST (Fig. 9b) ($P = 0.040$ and 0.014 , $r^2 = 0.22$ and 0.31 ; regression slope $a = 258$ and 1200 ; for MLD and MLI, respectively). The relatively low r^2 can be attributed to the large observation errors (as discussed above); nonetheless, the regression lines are statistically significant. This regression indicates a strong effect of Atlantic SSTs on the melting layer, which in turn is responsible for the formation and amount of freezing rain in the storms. For each degree Celsius increase of SST, an average increase of 258 m is observed in the MLD. The regression line slopes from RAMS are 115 and 760 for MLD and MLI, respectively (Fig. 10). It suggests that the observed sensitivity is greater than that predicted by

RAMS. Our simulations tested the effect of different SST forcing on a single test-case storm. It is possible that the SST changes can affect the synoptic-scale evolution of the storm in ways not simulated here. The MLD and MLI simulated with RAMS for this storm (in the control case, without SST offset) are close to the MLD and MLI that were measured at the time of the storm (Fig. 9). The difference can be attributed to the different horizontal and vertical grid resolutions at which the model calculations and radiosonde measurements were taken.

5. Conclusions

Heavy accumulation of freezing rain is the major cause of damage during ice storms in the southeastern United States (Jones et al. 2004). In general, the meteorological conditions that lead to ice storms along the southeastern U.S. coast, including the ice storm of 4–5 December 2002, are characterized by the combination of cold-air damming, which traps subfreezing air near the surface, and the transport of heat and moisture over the continent from the Gulf of Mexico and/or the west Atlantic, which leads to the development of the melting layer (Szeto et al. 1999; Robbins and Cortinas 2002). Using the December 2002 ice storm as a case study we find that warmer Atlantic SST increases the amount of heat and moisture transported in the melting layer, which is essential for the production of freezing rain. A

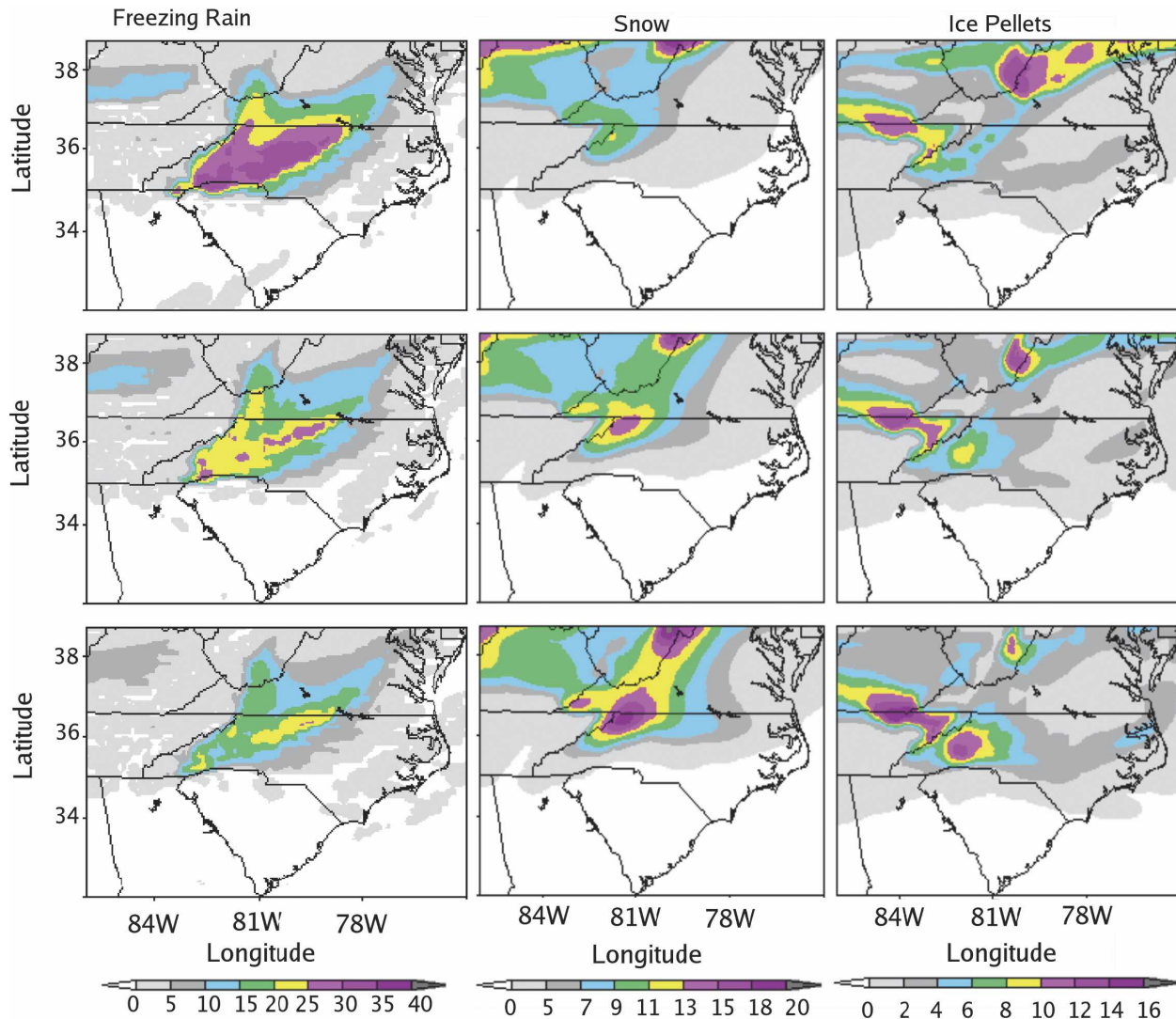


FIG. 8. Precipitation accumulation sensitivity simulated with RAMS for (top) SST +4°C, (middle) SST control, and (bottom) SST -4°C for (left) freezing rain, (center) snow, and (right) ice pellets.

deeper, warmer, and longer-lasting melting layer leads to an increased accumulation of freezing rain at the surface. This is also supported by Zerr (1997) and Stewart and King (1987), who found a similar connection between the melting layer and icing intensity.

Based on the RAMS simulations, we conclude that

while changes in SST do not significantly change the area subject to precipitation, they have a large impact on the amount of freezing rain. The simulations show that this effect is achieved through the increases of the MLD and MLI that result from elevated Atlantic SSTs. An even stronger sensitivity of the melting layer during

TABLE 2. Statistics of melting-layer (ML) criteria for ice/snowstorms in the observed storm-profile dataset. MLD is in km, and MLI is in km °C.

Station	No. of storms		Avg MLD		Avg MLI		% for ML > 0	
	Ice	Snow	Ice	Snow	Ice	Snow	Ice	Snow
Greensboro, NC	10	13	0.981	0.220	2.449	0.357	70.0%	15.4%
Sterling, VA	17	26	0.868	0.073	1.979	0.084	70.6%	14.3%

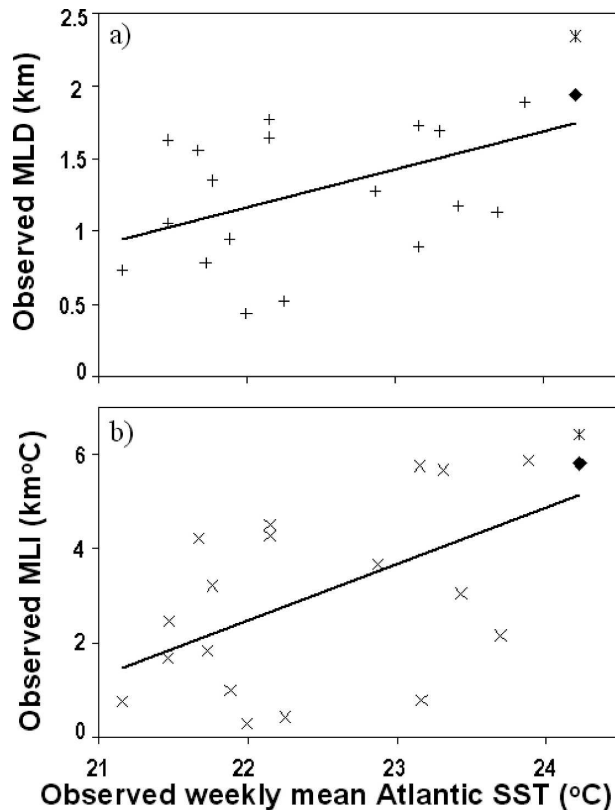


FIG. 9. Regressions between observed weekly mean Atlantic SSTs and (a) observed MLD (+ symbol) and (b) observed MLI (\times symbol). Observations include all ice storms between 1991 and 2004 that had a reported melting layer. The observations for the December 2002 ice storm are marked with an asterisk. The diamonds indicate the simulated result for the ice storm of December 2002 and were not included in the regression lines. Regression line equations: $MLD = 0.26 \times SST - 4.52$; $MLI = 1.12 \times SST - 23.91$; significance P equals 0.014 and 0.040; r^2 equals 0.31 and 0.22, for MLD and MLI, respectively.

storms over the southeastern United States to Atlantic SST is observed in ice storms during the last decade. Indeed, at two locations where simultaneous radiosonde observations and storm reports exist, the melting layer in storms since 1991 is positively and significantly correlated with Atlantic SST, with a stronger slope than the one suggested by the model simulations. Therefore, we suggest that the conclusions from the model simulations can be extended to ice storms of similar characteristics in the eastern United States, and that the Atlantic SST during synoptic events that generate winter storms plays a critical role in determining if and how much freezing rain the storm would produce, by affecting the MLD. A model that can include both global and regional scales such as the Ocean–Land–Atmosphere Model developed at Duke University (R. L. Walko and R. Avissar, unpublished manuscript) can simulate more

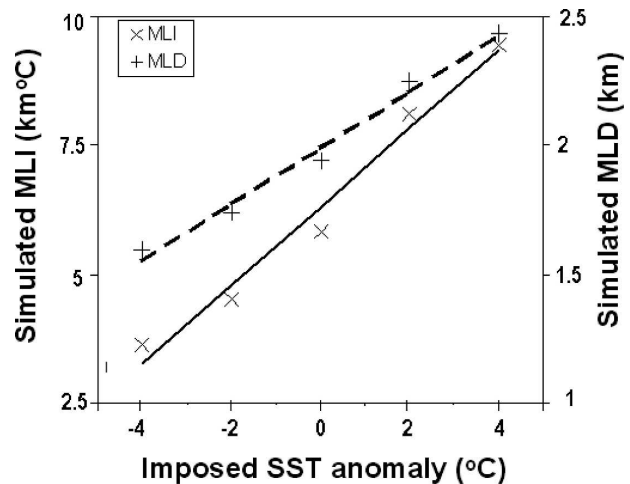


FIG. 10. Regressions between the Atlantic SSTs that were used to force RAMS and simulated MLD (+ symbol with scale on the right y axis) and MLI (\times symbol with scale on the left y axis). The data points represent the simulated MLD and MLI for five cases: the control run with average observed SST = 24.2°C , and four more simulated cases with -4° , -2° , $+2^{\circ}$, or $+4^{\circ}\text{C}$ offsets from the observed SST. MLI regression line (solid) equation is $MLI = 0.76 \times SST - 12.09$, $r^2 = 0.977$. MLD regression line (dashed) equation is $MLD = 0.11 \times SST - 0.65$, $r^2 = 0.986$.

accurately the interaction between the large-scale SST changes and the microscale dynamics of precipitation development.

The capability to correctly predict whether precipitation will occur as snowfall or freezing rain is a challenging problem with very significant implications for society given the devastating impacts of freezing rain. Our findings, which provide new insights on the physical mechanisms involved in these extreme weather events, emphasize that a high-resolution prediction model together with accurate SST can significantly improve our forecasting capability.

Acknowledgments. This research was supported by NASA under Grant NAG 5-9359 and by the NSF under Grant ATM-0346554. The views expressed herein are those of the authors and do not necessarily reflect the views of NASA or the NSF. We thank the anonymous reviewers who provided pertinent comments and suggestions on the original version of our manuscript. We recognize their invaluable contribution to this article.

REFERENCES

- Avissar, R., and R. A. Pielke, 1989: A parameterization of heterogeneous land surfaces for atmospheric numerical-models and its impact on regional meteorology. *Mon. Wea. Rev.*, **117**, 2113–2136.
- Bell, G. D., and L. F. Bosart, 1988: Appalachian cold-air damping. *Mon. Wea. Rev.*, **116**, 137–161.

- Bernstein, B. C., 2000: Regional and local influences on freezing drizzle, freezing rain, and ice pellet events. *Wea. Forecasting*, **15**, 485–508.
- Changnon, S. A., 2003a: Urban modification of freezing-rain events. *J. Appl. Meteor.*, **42**, 863–870.
- , 2003b: Characteristics of ice storms in the United States. *J. Appl. Meteor.*, **42**, 630–639.
- , and T. R. Karl, 2003: Temporal and spatial variations of freezing rain in the contiguous United States: 1948–2000. *J. Appl. Meteor.*, **42**, 1302–1315.
- DeGaetano, A. T., 2000: Climatic perspective and impacts of the 1998 northern New York and New England ice storm. *Bull. Amer. Meteor. Soc.*, **81**, 237–254.
- Forbes, G. S., R. A. Anthes, and D. W. Thomson, 1987: Synoptic and mesoscale aspects of an Appalachian ice storm associated with cold-air damming. *Mon. Wea. Rev.*, **115**, 564–591.
- Gyakum, J. R., and P. J. Roebber, 2001: The 1998 ice storm—Analysis of a planetary-scale event. *Mon. Wea. Rev.*, **129**, 2983–2997.
- Harrington, J. Y., 1997: The effects of radiative and microphysical processes on simulated warm and transition season arctic stratus. Atmospheric Department, Colorado State University, 288 pp. [Available from Dept. of Atmospheric Science, Colorado State University, Fort Collins, CO 80523.]
- Jones, K. F., A. C. Ramsay, and J. N. Lott, 2004: Icing severity in the December 2002 freezing-rain storm from ASOS data. *Mon. Wea. Rev.*, **132**, 1630–1644.
- Kalnay, E., and Coauthors, 1996: The NCEP/NCAR 40-Year Reanalysis Project. *Bull. Amer. Meteor. Soc.*, **77**, 437–471.
- Kocin, P. J., and L. W. Uccellini, 1990: *Snowstorms along the Northeastern Coast of the United States: 1955 and 1985*. *Meteor. Monogr.*, No. 44, Amer. Meteor. Soc., 280 pp.
- Kuo, Y. H., 1974: Further studies of the parameterization of the influence of cumulus convection of large-scale flow. *J. Atmos. Sci.*, **31**, 1232–1240.
- Louis, J. F., 1979: Parametric model of vertical eddy fluxes in the atmosphere. *Bound.-Layer Meteor.*, **17**, 187–202.
- Martner, B. E., J. B. Snider, R. J. Zamora, G. P. Byrd, T. A. Niziol, and P. I. Joe, 1993: A remote-sensing view of a freezing-rain storm. *Mon. Wea. Rev.*, **121**, 2562–2577.
- Mellor, G. L., and T. Yamada, 1974: A hierarchy of turbulence closure models for planetary boundary layers. *J. Atmos. Sci.*, **31**, 1791–1806.
- Meyers, M. P., R. L. Walko, J. Y. Harrington, and W. R. Cotton, 1997: New RAMS cloud microphysics parameterization. 2. The two-moment scheme. *Atmos. Res.*, **45**, 3–39.
- Pielke, R. A., and Coauthors, 1992: A comprehensive meteorological modeling system—RAMS. *Meteor. Atmos. Phys.*, **49**, 69–91.
- Reynolds, R. W., N. A. Rayner, T. M. Smith, D. C. Stokes, and W. Q. Wang, 2002: An improved in situ and satellite SST analysis for climate. *J. Climate*, **15**, 1609–1625.
- Robbins, C. C., and J. V. Cortinas, 2002: Local and synoptic environments associated with freezing rain in the contiguous United States. *Wea. Forecasting*, **17**, 47–65.
- Roebber, P. J., and J. R. Gyakum, 2003: Orographic Influences on the mesoscale structure of the 1998 ice storm. *Mon. Wea. Rev.*, **131**, 27–50.
- Stewart, R. E., and P. King, 1987: Freezing precipitation in winter storms. *Mon. Wea. Rev.*, **115**, 1270–1279.
- Szeto, K. K., A. Tremblay, H. Guan, D. R. Hudak, R. E. Stewart, and Z. Cao, 1999: The mesoscale dynamics of freezing rain storms over eastern Canada. *J. Atmos. Sci.*, **56**, 1261–1281.
- Walko, R. L., and C. A. Tremback, cited 2001: Introduction to RAMS 4.3/4.4. [Available online at www.atmet.com/html/docs/rams/ug44-rams.intro.pdf.]
- , W. R. Cotton, M. P. Meyers, and J. Y. Harrington, 1995: New RAMS cloud microphysics parameterization. Part I: The single-moment scheme. *Atmos. Res.*, **38**, 29–62.
- , and Coauthors, 2000a: Coupled atmosphere–biophysics–hydrology models for environmental modeling. *J. Appl. Meteor.*, **39**, 931–944.
- , W. R. Cotton, G. Feingold, and B. Stevens, 2000b: Efficient computation of vapor and heat diffusion between hydrometeors in a numerical model. *Atmos. Res.*, **53**, 171–183.
- Zerr, R. J., 1997: Freezing rain: An observational and theoretical study. *J. Appl. Meteor.*, **36**, 1647–1661.